research articles Journal of proteome research

Rapid Alteration of the Phosphoproteome in the Moss *Physcomitrella patens* after Cytokinin Treatment

Dimitri Heintz,*,† Anika Erxleben,‡ Anthony A. High,† Virginie Wurtz,† Ralf Reski,‡ Alain Van Dorsselaer,† and Eric Sarnighausen‡

Laboratoire de Spectrométrie de Masse Bio-Organique, CNRS, ECPM, Université Louis Pasteur, 25 rue Becquerel F67087, Strasbourg, Cedex 2, France, and Institute for Biology II, Plant Biotechnology, Faculty of Biology, University of Freiburg, 79104 Freiburg, Germany

Received April 7, 2006

Cytokinin hormones are crucial regulators of a large number of processes in plant development. Recently, significant progress has been made toward the elucidation of the molecular details of cytokinin that has led to a model for signal transduction involving a phosphorylation cascade. However, the current knowledge of cytokinin action remains largely unknown and does not explain the different roles of this hormone. To gain further insights into this aspect of cytokinin action and the inducible phosphorelay, we have produced the first large-scale map of a phosphoproteome in the moss *Physcomitrella patens.* Using a protocol that we recently published (Heintz, D.; et al. *Electrophoresis* **2004**, *25*, 1149−1159) that combines IMAC, MALDI-TOF-MS, and LC-MS/MS, a total of 172 phosphopeptide sequences were obtained by a peptide de novo sequencing strategy. Specific *P. patens* EST and raw genomic databases were interrogated, and protein homology searches resulted in the identification of 112 proteins that were then classified into functional categories. In addition, the temporal dynamics of the phosphoproteome in response to cytokinin stimulation was studied at 2, 4, 6, and 15 min after hormone addition. We identified 13 proteins that were not previously known targets of cytokinin action. Among the responsive proteins, some were involved in metabolism, and several proteins of unknown function were also identified. We have mapped the time course of their activation in response to cytokinin and discussed their hypothetical biological significance. Deciphering these early induced phosphorylation events has shown that the cytokinin effect can be rapid (few minutes), and the duration of this effect can be variable. Also phosphorylation events can be differentially regulated. Taken together our proteomic study provides an enriched look of the multistep phosphorelay system mediating cytokinin response and suggests the existence of a multidirectional interaction between cytokinin and numerous other pathways.

Keywords: phosphoproteomics • *Physcomitrella patens* • cytokinin • phosphorylation

Introduction

Phosphorylation is one of the most common and well-studied posttranslational protein modifications. Recent studies have demonstrated that cytokinin signaling exploits reversible phosphorylation modifications of proteins for signal transduction.[1−3] However, the current knowledge of cytokinin signaling does not explain all of the pivotal roles of this phytohormone in plants. Indeed cytokinin is known to promote growth, cell division, chloroplast division, senescence delay, nutrient mobilization, and mediation of a number of light-regulated processes such as de-etiolation and chloroplast maturation.[1,2] For the most part, signal propagation for these well established cytokinin effects remains poorly understood.

In recent years, it has been shown that the moss *Physcomitrella patens* (*P. patens*) provides a suitable model to study cytokinin signaling since it is one of the few plant systems where cytokinin-induced differentiation can be studied at the single-cell level.[4−6] Additionally *P. patens* is unique among plants in its ability to incorporate DNA very precisely at predefined genomic loci (homologous recombination), allowing gene knock-outs similar to the ones performed in yeast and embryonic mouse cells.[7−10] Furthermore, *P. patens* is one of the oldest land plants and has not changed much during 450 million years and therefore contains some unique genes that have likely been lost in other plant species during their evolution.[4,8] Finally, *P. patens* can be cultivated in bioreactors providing large-scale production under highly standardized conditions that involve tight control of plant growth and differentiation, thus allowing proteomic studies in a reproducible manner.[11,12]

* To whom correspondence should be addressed. Tel: +33 (0)3 90 24 26 81. Fax: +33 (0)3 90 24 27 81. E-mail: dheintz@chimie.u-strasbg.fr.
† CNRS, ECPM.
‡ University of Freiburg.

10.1021/pr060152e CCC: $33.50

Immobilized metal affinity chromatography (IMAC) using Fe(III) as the ligand is highly useful for the enrichment of phosphopeptides from complex mixtures.[13−15]

IMAC has enabled mass-spectrometry-based phosphoprotein and phosphoproteome analysis in a variety of organisms, including yeast, humans, and, to a lesser extent, plants.[16−19,20−22]

However, large scale mapping of phosphoproteins gives only a partial picture of signaling dynamics. Therefore, temporal studies of early phosphorylation events induced specifically in response to a stimulus are of particular interest from a biological point of view. For example, in a recent report, 81 proteins belonging to the human epithelium growth factor (EGF) signaling pathway were identified.[16] A recent study done in yeast described 139 phosphorylated proteins that were differentially regulated in response to a mating pheromone.[23] Plant global dynamic studies of phosphorylation-based early signaling events in response to a stimulus have not been widely published to date. Here, in this report, we have produced the first large-scale map of phosphorylated proteins and a temporal dynamics profile of cytokinin signaling by deciphering the early phosphorylation events that occur during the first 15 min after cytokinin stimulation in *P. patens*. We have previously reported a method for large-scale phosphopeptide purification from complex protein mixtures in *P. patens,* combining RP-HPLC, IMAC, alkaline phosphatase treatment, MALDI-TOF-MS, LC-MS/MS, and peptide de novo sequencing.[24] The classical approach for peptide identification, which consists of scoring the mass spectrum obtained by LC-MS/MS against a database of all candidate peptides to detect significant matches, requires that the genome be accurately sequenced and all protein coding genes annotated.[25] Since the *P. patens* genome has not yet been fully sequenced and is only available as expressed sequence tags (EST) and a set of raw genomic data, a de novo sequencing strategy was necessary to allow successful protein identification. This strategy involves the manual treatment of the peptide fragmentation LC-MS/MS mass spectra to deduce a complete or partial peptide sequence tag.[26]

The peptide sequences determined this way are then submitted to a BLAST program that allows the interrogation of existing *P. patens* EST and raw genomic data. The ESTs were then used as query to interrogate the NCBI protein database in order to identify proteins by homology searches. Thus, in this study, we have produced the first large-scale map of phosphorylated proteins from a whole *P. patens* cell lysate. Additionally, we analyzed the temporal changes of phosphorylation that occur within a time course of 15 min after cytokinin stimulation. We identified 13 proteins which were not previously known to be targets of early phosphorylation events in response to cytokinin stimulation. The biological significance of these 13 proteins as well as the mechanism by which cytokinin mediated phosphorelay may occur is described and discussed in this paper.

Results and Discussion

Starting from a whole *P. patens* protein tryptic digest, a total of 179 peptide sequences were obtained by de novo peptide sequencing using LC-MS/MS spectra (Table 1, Supporting Information). The combination of MALDI-TOF-MS profiling and alkaline phosphatase treatment highlights the specificity of our IMAC-based phosphopeptide isolation strategy. Indeed among the 179 peptides identified, 172 (representing 96.1%) responded positively to alkaline phosphatase treatment and therefore were considered to be phosphorylated peptides (Table 1, Supporting Information). Only 7 peptides (representing 3.9%) of the 172 peptides were not responsive to alkaline phosphatase treatment and thus considered to be nonphosphorylated peptides. We could not determine conclusively from our experiments whether the 7 peptides that did not respond to alkaline phosphatase treatment bound nonspecifically to the IMAC matrix, lost their phosphate groups prior to alkaline phosphatase treatment, or displayed resistance toward enzymatic dephosphorylation.[27] From the 172 phosphorylated peptides, 78 were unambiguously monophosphorylated (45.3%) and 94 were multiphosphorylated peptides (54.7%). Surprisingly, the number of multiphosphorylated peptides enriched was higher than the monophosphorylated peptides, and this result seems to be a characteristic of IMAC−Fe3+ principle, since several authors have observed this phenomenon in different phosphoproteomics studies.[23,28] The use of the *P. patens* single phosphopeptide tag for the determination of the *P. patens* ESTs was revealed to be largely successful as reported earlier.[24] Thus, in the present study, among the 179 peptide tags, we succeed with 169 peptide sequences using a tBLASTn approach in the determination of the ESTs (Table 1, Supporting Information). However, some limitations exist: for example, BLAST searches failed when MSMS spectra were not sufficiently informative and consequently peptide sequences obtained by de novo sequencing were too short (Table 1 “No BLAST”, Supporting Information).

As a way to highlight the presence of phosphopeptides and assign phosphorylation sites on the different fractionated phosphopeptides, we attempted direct sequencing of the phosphopeptides by MALDI-TOF-MS/MS and LC-MS/MS, LIFT, and CID in the reflectron positive and negative mode. The negative mode was characterized by a high decrease of the global signal intensity (data not shown). The MS and MS/MS spectra obtained in the positive mode were characterized by the neutral loss of 98 or 80 Da from the simply charged precursor characteristic of phosphoserine and phosphothreonine peptides (data not shown). These diagnostic ions are used to unambiguiously distinguish phosphorylated peptides from nonphosphorylated peptides.[29,31] However, in our study, the phosphopeptides MS/MS spectra obtained were often not sufficiently informative to enable manual reconstruction of the peptide sequence (bold amino acid sequences Table 1 and Supporting Information, Table 1). Indeed it is well-known that the increased acidity of the phosphate group generally results in decreased ionization efficiency of a peptide.[30,31] We therefore sequenced the phosphorylated peptides after having been dephosphorylated by alkaline phosphatase treatment by MALDI-TOF-MS/MS and LC-MS/MS, and thereby we obtained larger peptide sequences (Table 1 and Figure 6 in the Supporting Information). However, this strategy needed some additional verifications to control the peptides that were fragmented by LC-MS/MS, following a MS and MS/MS priority sequencing list (see Materials and Methods section) correspond really to the peptides which we identified as being phosphorylated by MALDI-TOF-MS (peptides whose mass shifted following phosphatase treatment). Therefore, we controlled systematically visually the LC−UV and MS run profiles and checked the precursor ions which have been selected for MSMS. Additionally, we compared the amino acid sequences obtained by MALDI-TOF-MS, MS/MS LIFT, and CID with the amino acid sequences obtained by LC-MS/MS. Thus, all of the amino acids obtained by phosphopeptide fragmentations using MALDI-TOF−MS/MS and LC-MS/MS could be found in the corre-

Table 1. List of the 13 *P. patens* Proteins Responsive to Cytokinin Treatment at Different Time Points after Stimulation

HPLC fraction[a]	MS mass (*m*/*z*) [M+H]+	protein descripiton	phosphopeptide (partial) sequence obtained by de novo sequencing[b]	species	GI number (NCBI)	*E* value[c]	*P. patens* EST/ contig/ raw genomic sequence no.[d]	phosphorylation state		phosphorylation previously determined
								cytokinin +	cytokinin −	
				2 min after stimulation						
7	2171.0	MOPP 1	YSKP**HGWP**	*Physcomitrella patens*			AW739428	3	≠3	
3	2155.1	MOPP 2	S*YAEWA**EEGK**	*Physcomitrella patens*			PP_17759_C1	2 (8X increase)	2	
3	1668.7	MOPP 3	VYDAG**DGAK**	*Physcomitrella patens*			PP001075088R	1	≠1	
3	1214.6	rubisco large subunit	DDY*I**E**KDR	*Physcomitrella patens*	14861091	0.0		2	≠2	
5	1475.2	serine hydroxymethyl-transferase	**VAE**YFDR	*Pisum sativum*	169158	1e-168	PP_176_C5	1	≠1	
				Arabidopsis thaliana	17979462	1e-49	BJ591938			
				Pisum sativum	169158	2e-30	BJ173131			
4	1460.4	sedoheptulose-1,7-bisphos-phatase	**FEE**T*LY*GDSR	*Arabidopsis thaliana*	15451178	4e-73	PP_SD_143_C1	1	≠1	
				4 min after stimulation						
1	1118.6	MOPP 4	DTDLA**QAFR**	*Physcomitrella patens*			PP_4706_C3	1	≠1	
2	2361.0	MOPP 5	YAPENESA-**GGA**GYR	*Physcomitrella patens*			not found	3	≠3	
3	1290.6	MOPP 6	TAS*L**GDR**	*Physcomitrella patens*			PP_14772_C1	1	≠1	
3	2155.1	MOPP 2	S*YAEWA**EEGK**	*Physcomitrella patens*			PP_17759_C1	2 (8X increase)	2	
9	2042.0	methionine synthase	IS*E**E**DY*DK	*Hordeum vulgare*	68655500	0.0	PP_304_C2	2 (3−6X increase)	2	
				6 min after stimulation						
8	877.5	carbonic anhydrase isoform 1	DSALFDK	*Gossypium hirsutum*	4754913	1e-29	PP011003042R	1 (5X increase)	1	
						8e-41	PP004069260R			
						7e-23	PP_403_C10			
9	2042.0	methionine synthase	IS*E**E**DY*DK	*Hordeum vulgare*	68655500	0.0	PP_304_C2	2 (3−6X increase)	2	
7	1471.6	glyceraldehyde-3-phosphate dehydrogenase	TFAEEVNQAFR	*Sphagnum cuspidatum*	18076108	5e-88	PP004107162R	2	≠2	(63)
				Marchantia polymorpha	18076100	5e-80	PP_325_CB5			
				Spinacia oleracea	2529370	1e-132	PP_73_CB11			
				15 min after stimulation						
9	2042.0	methionine synthase	IS*E**E**DY*DK	*Hordeum vulgare*	68655500	0.0	PP_304_C2	2 (3−6X increase)	2	
1	1718.6	oxygen-evolving enhancer protein 2	**FLDE**VSY*LFGK	*Arabidopsis thaliana*	6692695	3e-55	BI437128	2	≠2	(64)
				Solanum tuberosum	1771778	1e-74	PP_1032_C7			
				Arabidopsis thaliana	6692695	2e-70	PP_370_C1	PP_370_C1	PP_370_C1	PP_370_C1
2	1198.7	MOPP 7	**GDE**VPGH	*Physcomitrella patens*			BJ605312	≠ 1	1	
							PP004083078R			
							PP_48_CB5			
				PP_48_CB5	PP_48_CB5	PP_48_CB5	BJ161355			

[a] The numbers 1−10 correspond to the HPLC fraction which contains the phosphopeptide analyzed. [b] The partial peptide sequences resulted from de novo sequencing using nano LC-MS/MS M spectra. In bold are the sequences obtained by MALDI-TOF-MS/MS using LIFT and CID fragmentation mode on the phosphorylated peptides. [c] The expected value of the *P. patens* ESTs, contigs, or genomic data. The peptide sequence tag has been used to interrogate the *P. patens* EST, contig, and genomic available raw sequences databases (http://www.cosmoss.org/. ftp://ftp.ncbi.nih.gov/pub/TraceDB/Physcomitrella_patens/). The phosphorylated peptideis are indicated by the mono charged peptide mass $[M+H]^+$. The proteins were identified by homology searches on NCBI. The protein database was interrogated using as query the identified *P. patens* EST, contig, and genomic available raw sequences data. The gene info identifier (GI) number of the protein from the species identified on NCBI. The phosphorylated and dephosphorylated states are shown and have determined by MALDI profiling before/after alkaline phosphatase treatment. The phosphorylated proteins for which the phosphorylation state involves a stronger recruitment of that protein for a particular phosphorylation state in response to cytokinin are labeled in parentheses by the factor of increase/decrease. MOPP "MOss Phosphorylated Protein" represent *P. patens* peptides from which the corresponding EST, contig, and raw genomic sequences shared no homology to any organism in the current nonredundant protein database maintained by the NCBI. The identified phosphopeptides have been evaluated by NETPHOS 2.0 (www.cbs.dtu.dk/services/Net-Phos) and phosphorylated amino acids are labeled (*).

sponding dephosphorylated peptide sequences (Supporting Information, Table 1). These precautions were taken to regard the list of phosphorylated peptides given in this study as validated.

Proteomic Analysis Validates *P. patens* as a Rich Source of Moss Phosphorylated Proteins (MOPP). In the present study, we identified 112 proteins (Figure 1). As a result, we could show that 30.0% of *P. patens* ESTs/contig or raw genomic

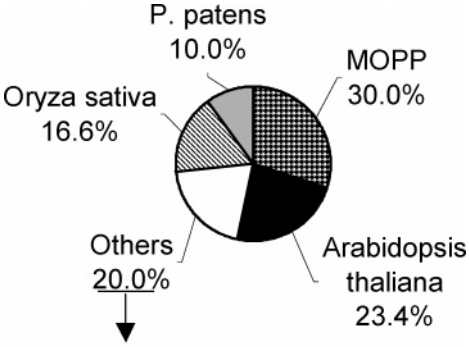

Hyacinthus orientalis	2.5%
Solanum tuberosum	1.87%
Nicotiana plumbaginifolia	1.25%
Spinacia oleracea	1.25%
Arachis hypogaea	0.62%
Caenorhabditis elegans	0.62%
Chlamydomonas reinhardtii	0.62%
Cicer arietinum	0.62%
Hevea brasiliensis	0.62%
Triticum aestivum	0.62%
Lycopersicon esculentum	0.62%
Medicago truncatula	0.62%
Mesembryanthemum crystallinum	0.62%
Petroselinum crispum	0.62%
Pinus pinaster	0.62%
Pisum sativum	0.62%
Phaseolus vulgaris	0.62%
Prunus dulcis	0.62%
Solanum demissum	0.62%
Zantedeschia aethiopica	0.62%
Zea mays	0.62%
Nicotiana tabacum	0.31%
Cryptococcus neoformans	0.31%
Daucus carota	0.31%
Gossypium hirsutum	0.31%

Figure 1. Distribution of *P. patens* phosphorylated proteins by homology searching. The proteins listed in Table 1 of the Supporting Information have been classified by their homology to other species. 30.0% were *P. patens* proteins that shared no homology to any organism in the current National Centre for Biotechnology Information (NCBI) nonredundant protein database. These proteins were therefore named MOPP "MOss Phosphorylated Protein". 23.4% of the *P. patens* ESTs, contigs, or raw genomic data were homologous to *Arabidopsis thaliana* proteins; 16.6% were homologous to *Oriza sativa* proteins; 20% were homologous to 25 additional organisms termed "others" and listed in the table below the pie chart.

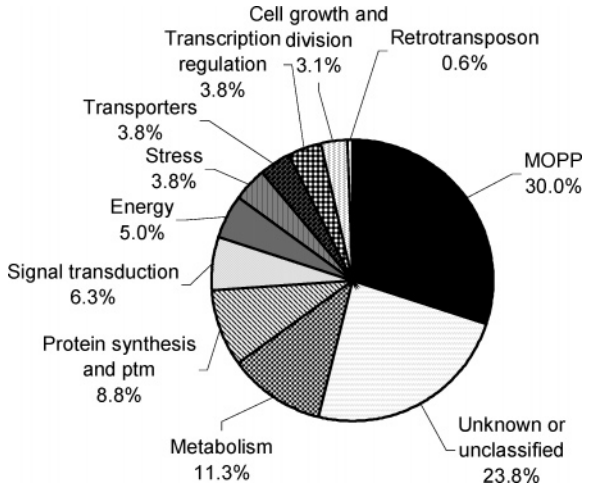

Figure 2. Distribution of *P. patens* phosphorylated proteins by putative similar function. The proteins listed in Table 1 of the Supporting Information have been grouped into different functional categories. The protein function assignment was made according to homology search results in NCBI and completed by InterPro (http://www.ebi.ac.uk/interpro/) and Pfam (http://www.sanger.ac.uk/Software/Pfam/ind ex.shtml). MOPP "MOss Phosphorylated Protein" represent *P. patens* proteins from which the corresponding EST, contig, and raw genomic sequences shared no homology to any organism in the current nonredundant protein database maintained by the NCBI.

sequences have no homology to any other organism in the current publicly accessible databases. Thus, we named these proteins MOPP for "MOss Phosphorylated Proteins". Different predictive bioinformatic tools have been tested, but these have not permitted us to conclude any hypothetical function for these proteins. Thus, we can only propose to date that these proteins are phosphorylated in *P. patens*. We are aware that we cannot exclude the fact that similar MOPPs may exists in other organisms different from *P. patens* but that are not yet present in the current protein databases and therefore would not have shown up as hits during our searches. We can also not exclude that MOPPs are specific to *P.* patens. Indeed this hypothesis of "moss specificity" can be supported and might not be excluded since *P. patens* is one of the oldest land plants and has not changed much during 450 million years of evolution as reported by different authors.[32−34] Therefore, *P. patens* should contain unique genes that have been lost in other plant species during their evolution.[32−34] Indeed, of the 25 000 estimated *P. patens* genes, 5000 may be unknown expressed genes unique to that organism.[32−35] Our protein homology search data revealed that the *P. patens* proteins are largely homologous to higher plants (Figure 1), especially to *Arabidopsis thaliana* (23.4%). Rice appeared as the second most homologous species, whereas 20% of the *P. patens* phosphoproteome is homologous to a group of 25 different species from which 23 are different plants. Additionally, the results of protein functional classification attempted in our study provided information that the *P. patens* phosphoproteome contains a set of proteins shared with different higher plants but with unknown function (23.8%; Figure 2). Interestingly, most of the homologue proteins are not known to be phosphorylated in the different species; therefore, we cannot conclude if phosphorylation is conserved from one species to the other. The new information provided here is that these *Physcomitrella* proteins are phosphorylated, and it would be interesting in the future to know if similar proteins are also phosphorylated in other species. Nevertheless, this result strongly suggests that plant communication circuits based on phosphorylation events remain complex and largely unknown. Our study has indicated that phosphorylation events in *P. patens* are largely involved with metabolism (11.3%, Figure 2). We can hypothesize that protein phosphorylation plays an important role in the regulation of metabolic activity in *P. patens*. *Physcomitrella* is known to contain an extremely high percentage of genes involved in metabolism (73%) compared to other plants which might be explained by a lot of alternative metabolic pathways not known from seed plants.[36]

Cytokinin-Induced Phosphorylation Events Are Rapid and Nearly Complete in 15 min. Up to now, temporal changes in phosphorylation have not been studied in the cytokinin signaling pathway. Here we report phosphopeptide profiling in

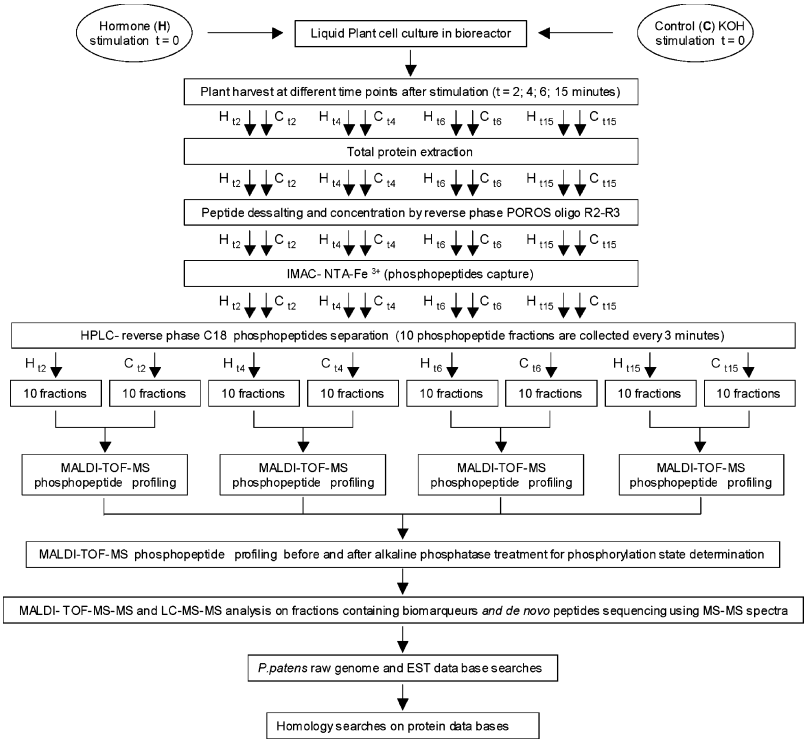

Figure 3. Schematic illustrating the strategy used for phosphopeptides profiling and identification and characterization of phosphorylated proteins responsive to cytokinin.

response to cytokinin at different time points after the stimulation (Figure 3). MALDI-TOF−MS peptide profiling exhibits several advantages such as automation, speed, sensitivity, reproducibility, and relative quantitation at the low femtomole level.[37] MALDI-TOF−MS phosphopeptide profiling and relative quantitation in combination with alkaline phosphatase treatment permitted to identify 13 phosphopeptides specifically altered in response to cytokinin (Figure 4). One significant outcome of our study is that the number of phosphopeptides responsive to cytokinin was elevated immediately (two minutes) after hormone stimulation, reached a maximum 4 min after the stimulation, and decreased to a minimum 15 min after stimulation. This data shows that cytokinin signal propagation mediated through phosphorylation events can occur extremely rapidly in *P. patens*. In line with that observation are some known cytokinin effects that have been reported recently which are all rapid, e.g. 3 min after cytokinin addition to a plant suspension culture. These include the release of NO molecules indicating involvement of a rapid NO-dependent signaling system.[38] Signal "run-on" experiments revealed that cytokinin induced the expression of the *Arabidopsis* response regulator (ARR) genes after 5 min and that maximal expression was detected after 10 min, accompanied by rapid termination of this effect after 20 min.[39] Recently, a genome-wide expression profiling has shown that 15 min after cytokinin treatment on *Arabidopsis* seedlings 82 genes were responsive to the hormone.[40] It is therefore conceivable that protein phosphorylation mediated by cytokinin must be rapid since several authors reported gene expression under cytokinin control within 15 min after the cytokinin pulse.[39,40]

Thirteen Proteins Respond to Cytokinin Stimulation by Temporal Changes in Their Phosphorylation Pattern. The 13 phosphopeptides altered in responsive to cytokinin action permit us to identify and characterize 13 proteins responsive to cytokinin (Supporting Information, Table 1). Interestingly, none of these proteins were previously known to be linked to cytokinin signaling. This new finding is evidence that the cytokinin-induced phosphorelay involves more proteins than the current view of the phosphorelay proposes. Our result is in line with reports of several authors indicating the existence of an alternative mechanism of cytokinin coexisting with the canonical phosphorelay of the two-component system mediating cytokinin signaling.[40−42] Interestingly, none of the known members of the two-component cytokinin signaling pathway were identified in our work. This result is not surprising and was anticipated since all proteins from the two-component pathway are phosphorylated on histidine and aspartic acid residues[42] that are labile in acidic or basic conditions.[43] In our proteomic approach, we made no special effort to modify conditions to preserve phosphate groups that may have resided on histidine or aspartic acid amino acids.

Some of the Proteins Responsive to Cytokinin Are Plastids Proteins. Our study showed that among the 13 proteins responsive to cytokinin 4 are known members of metabolic pathways or key enzymes of the chloroplast energy conversion machinery (rubisco large subunit, sedoheptulose-1,7-bisphosphatase, carbonic anhydrase isoform 1, oxygen-evolving enhancer protein 2; Figure 5). This result shows that cytokinin affects phosphorylated proteins of the *P. patens* plastome. The fast response of plastid phosphorylated proteins to a cytokinin signal is very important information. To our knowledge, this is the first report indicating that several plastid proteins can rapidly be altered at the level of phosphorylation in response to cytokinin. Numerous reports show that plastids are primary targets of cytokinin action.[42,44,45] Indeed it is largely acknowledged that cytokinins control chloroplast biogenesis and differentiation.[42,44,45] In a recent report, the fast response of plastid genes (within 15 min) to cytokinin was shown, and the authors

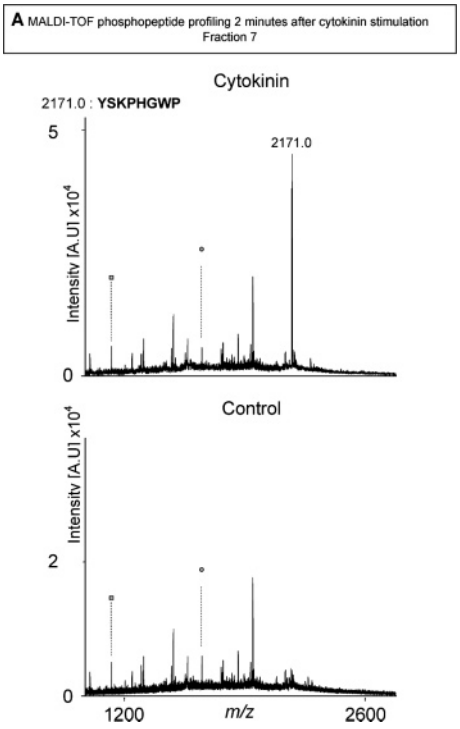

Figure 4. MALDI-TOF-MS phosphopeptide profiling of cytokinin stimulated and control fractions. (A and B−M Supporting Information) These figures show phosphopeptide patterns at different time points after cytokinin stimulation (2, 4, 6, and 15 min) as compared to the corresponding control (nontreated fractions). The phosphopeptides were purified by IMAC and the phosphopeptide mixture was separated by RP-HPLC into 10 fractions. These 10 fractions were collected and then a comparison was made between cytokinin treated and the corresponding control fractions. The MS spectra represent the phosphopeptides that were altered in response to cytokinin stimulation and their corresponding monoisotopic masses $[M+H]^+$ are indicated. Ring and square labeled peaks represent the peptides used as internal standards for the relative quantisation ($[M+H]^+ = 1645.8076$; $[M+H]^+ = 1125.4941$).

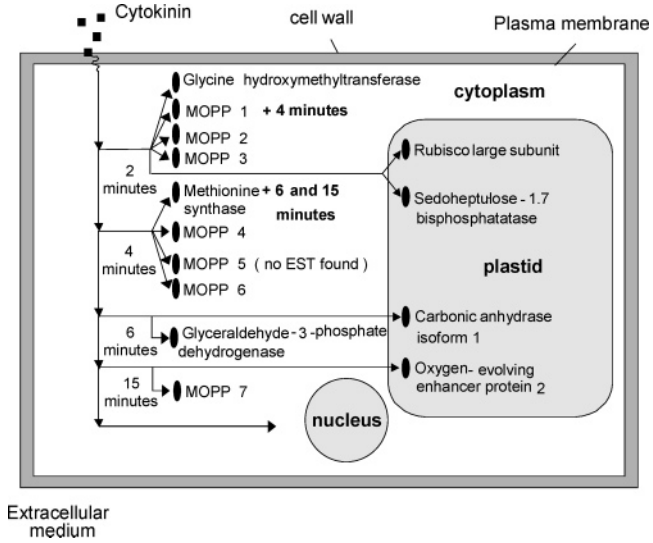

Figure 5. Schematic illustrating the localization in the cell of 13 *P. patens* phosphoproteins that were identified and determined to be responsive to cytokinin at different time points after stimulation (2, 4, 6, and 15 min). The rings indicate the cellular localization of the phosphoprotein based on the information provided by the function of the corresponding homologous protein and different bioinformatics prediction tools. MOPP "MOss Phosphorylated Protein" represents *P. patens* peptides from which the corresponding EST, contig, and raw genomic sequences shared no homology to any organism in the current nonredundant protein database maintained by the NCBI.

hypothesize that the plastids may be partially autonomous with respect to their cytokinin response.[40] A specific route of phosphorelay cytokinin action for chloroplasts might therefore also be an explanation for rapid signal transfer to plastids we observe in our study. Among the different chloroplast proteins responsive to cytokinin and identified in our work are some that are involved in light signaling (rubisco large subunit, oxygen evolving enhancer protein 2, sedoheptulose-1,7-bisphosphatase). The possible involvement of these key enzymes of the chloroplast energy-conversion machinery in organelle division and cellular differentiation has been discussed previously.[5] The cross-talk between cytokinin and light signaling pathways has been reported by several authors.[46−48] Recently, it has been shown that elevated cytokinin doses can even mimic the phenotype of constitutive photomorphogenic (de-etiolated) mutants[49], i.e., mutants that display a light-grown morphology in darkness. A recent report has shown that the response regulator 4 protein (ARR4), a possible mediator of cytokinin action, interacts directly with phytochrome B and stabilizes its active form.[48] In summary, physiological experiments and mutant analyses suggest a link between hormone and light signaling pathways; however, the mechanistic basis of this cross-talk is still poorly understood.[47,48] A plastid carbonic anhydrase was identified as a cytokinin target protein (Table 1) indicating that cytokinin action is linked to CO_2 metabolism. Recently, it was reported that increases of the CO_2 concentration in cotton leaves have the effect of increasing cellular cytokinin concentration and an elevated photosynthetic activity was observed. It was also hypothesized that elevated CO_2 stimulates cells to divide.[50] Additionally CO_2 is known to be a substrate for Rubisco (involved in photosynthetic activity). It is therefore conceivable that cytokinin action on carbonic anhydrase has a consequence in the variation of cellular CO_2 flux leading to an increase of photosynthetic activity. Taken together, our data showing key chloroplast proteins as targets of cytokinin action suggests that cytokinin can regulate plant photosynthetic activity and energy-conversion machinery by controlling the activity of plastid proteins by modifying their phosphorylation states and levels.

Cytokinin Action Is Complex. The different functional categories of the cytokinin target proteins (Figure 5) highlight the multiple pathways in which cytokinin action takes place in *P. patens*. We have previously described proteins implicated in light signaling and photosynthesis, including some proteins involved in different metabolisms (glycine hydroxymethyltransferase, methionine synthase, glyceraldehyde 3-phosphate dehydrogenase), and glycine hydroxymethyltransferase and methionine synthase, which both are enzymes in the primary metabolism involved in amino acid synthesis.[51−53] A link between cytokinin and amino acid synthesis has to our knowledge not been previously described. Regulation of protein synthesis and turnover is important in plants and may be expected to be relevant for cytokinin function, although little experimental evidence has been published to date.[54] Since cell growth is promoted by cytokinin as an accompaniment to biomass production, we can hypothesize that it also has an

effect on protein turnover and therefore a possible involvement with these key enzymes**.** A glyceraldehyde 3-phosphate dehydrogenase (GAPDH) cytokinin target protein was identified in our work (Table 1). This enzyme is involved in sugar metabolism and displays diverse nonglycolytic functions depending upon its subcellular location.[55−57] The relationship between cytokinin and sugar metabolism has been reported by different authors, although the full physiological relevance of this role remains unclear.[38,58] Recently, it was shown that plants with impaired cytokinin receptors CRE1 and AHK3 display increased sugar sensitivity. The authors suggested the existence of a bidirectional antagonist interaction between sugars and cytokinins.[58] In addition, it is plausible that GAPDH is a target of cytokinin action as a way to regulate glycolytic activity by modifying the phosphorylation state of GAPDH.

Our study has shown that several moss phosphorylated proteins (MOPP) are also cytokinin target proteins (Figure 5). Due to the absence of homologous proteins in the current databases, we are not able to conclude that MOPPs are exclusively involved in a specific *P. patens* cytokinin signaling pathway. However, we cannot exclude that other species share MOPP proteins as it was described earlier in this paper. These results indicate that a large part of cytokinin target proteins remains a mystery with regard to their function.

Additionally, we observed from MALDI-TOF-MS phosphopeptide profiling that cytokinin can affect phosphorylation in different ways (Figure 4).

Indeed we observed at the peptide level that a change of phosphorylation state in response to cytokinin stimulation can occur (Figure 4). Thus, for 10 of the 13 proteins responsive to cytokinin, the effect is characterized by a change in the phosphorylation/dephosphorylation state in response to the hormone pulse, (see e.g., MOPP, 1, 3, 4, 5, 6, and 7, glycine hydroxymethyltransferase, methionine synthase, glyceraldehydes−3-phosphate dehydrogenase (Table 1)). The change of phosphorylation state is characterized by peaks present exclusively in phosphopeptide profiles of the cytokinin-treated fractions compared to the absence of corresponding peaks in the control phosphopeptide profiles and vice versa.

Additionally, we have also observed that cytokinin can affect the phosphorylated to nonphosphorylated ratio of particular peptides. For these peaks, the m/z value is the same in control and cytokinin phosphopeptide profiles but the intensity varies between cytokinin treated and control phosphopeptide profiles (see e.g., MOPP 2, the methionine synthase, and the carbonic anhydrase protein, Table 1). Our results show that temporal changes in phosphorylation can be differentially modulated by cytokinin. However, at this level, we cannot exclude that the limits of sensitivity of our approach, explain that diminished phosphorylation below a certain threshold cannot be determined.

Finally, an additional degree of complexity in the cytokinin mechanism of phosphorylation modulation has been highlighted in our study. Indeed the variable duration of cytokinin phosphorylation modulation on its different target proteins was determined (Table 1, Figure 5). For 11 of the 13 proteins responsive to cytokinin, the duration of the signal does not exceed 2 min following activation. At this stage, we cannot exclude that the duration of the signal is prolonged and remains under the limit of detection. Additionally, due to the numerous samples to analyze simultaneously, we have not studied phosphorylation events in response to cytokinin before 2 min or after 15 min. However, for MOPP 2 and the methionine synthase, the cytokinin effect is maintained several minutes (Figure 5). Taken together these multiple levels of phosphorylation modulation/regulation contribute to the complex network of mechanisms that characterize cytokinin action.

In conclusion, our proteomic study has provided the first large-scale phosphoprotein map in *P. patens* and therefore shows a view of the global organization of the phosphoproteome.

Indeed the data presented here demonstrates that the seedless *P. patens* phosphoproteome is composed largely of proteins homologous to higher plants. It suggests that the organization of the phosphoproteome in *P. patens* might have a similarity to that of higher order plants, but unfortunately, a comparative study made in a higher plant has not yet been done. Our data also shows that the cytokinin-activated phosphoproteome is largely composed of proteins with unknown function as well as of proteins not present in the current protein database (MOPP). Clearly, this finding shows that the role and importance of phosphorylation in the plant cell remains poorly understood. Additionally, we have taken particular interest to study the global dynamics of the phosphoproteome in response to cytokinin stimulation. We devised a proteomic strategy to enable global, time-dependent analysis, and we studied the early phosphorylation events that occur in response to cytokinin stimulation within a period of 15 min. One significant outcome of this study is the finding of 13 novel early cytokinin-responsive target proteins that were not previously known to be associated with cytokinin action. This result indicates that cytokinin action may not exclusively involve phosphorylated proteins from the two-component system for mediating the cytokinin response. Here we provide direct evidence that an alternative pathway exists. The temporal order of the different participants in the cytokinin signaling as well as the magnitude of their activation was determined and was shown to be variable from one target protein to the other. Our data has shown that cytokinin action is involved in numerous cellular pathways. An important result in our study is the clear evidence that cytokinin-induced phosphorelay can rapidly occur in plastids. With the rapidity of the phenomenon observed, we can hypothesise a specific route of cytokinin action to the plastids.

In light of the findings reported here, one can readily conclude that cytokinin action is complex, but our data helps to provide a better understanding of it and its mechanism. We have demonstrated a viable framework for further investigations of the mechanisms plants use to mediate cytokinin response, which will allow us to advance our knowledge of the many biological processes governed by cytokinin. More broadly, the protocol used in our report is robust and our methodology is established, allowing our temporal analysis to be extended to many other organisms, time courses, other hormones, or stress conditions.

Experimental Section

Materials. Urea (electrophoresis reagent), 3-[(3-cholamidopropyl)-dimethylammonio]-1-propane sulfonate (CHAPS), 6 (γ-γ)dimethylallylaminopurine (2iP, Sigma-Aldrich Chemie Gmbh) were from Sigma-Aldrich (St Louis, MO). Trifluoroacetic acid, tributyl phosphine (TBP), and iron(III) chloride hexahydrate were from Fluka (Buchs, Swizerland). Sequencing grade modified trypsin was from Promega (Madison, WI) and alkaline phosphatase (1×10^3 U/mL) was from Roche Applied Science (Mannheim, Germany). Reversed phase packing POROS 50 R2

was from PerSeptive Biosystems (Framingham, MA) and oligo R3 reversed phase packing was from Applied Biosystems (Foster City, CA). IMAC material, Ni−NTA Superflow, was from Qiagen (Hilden, Germany). MALDI matrix a-cyano-4-hydroxycinnamic acid (HCCA) was from Sigma-Aldrich. MS calibration standards were from Sigma-Adrich. All other chemicals were reagent grade. All solutions were prepared with HPLC grade water.

Growth of Plant Material. *P. patens* (Hedw.) B. S. G. was grown in liquid modified Knop's medium as previously described.[11] The protonema cultures were run in semi-continuous bioreactors.[12] For time course analysis, the bioreactor material was taken when the dry weight reached, 150 mg/L corresponding to six-day-old bioreactor culture. The plant material was harvested from 4 L of culture medium by filtration and transferred to 6 L balloon flasks containing 4 L of fresh Knop medium. The culture homogeneity was kept constant by continuous stirring on a magnetic agitator while 150 mL of moss medium was transferred to 180 mL Erlenmeyer flasks. The cultures were grown while agitated for 17 additional hours under standard conditions described above, until hormone treatment. The overall procedure was conducted under sterile conditions.

Hormone Treatment and Time Course Procedure. The protonema cultures were treated either with cytokinin 6 (γ-γ) dimethylallylaminopurine (2iP) to a final concentration of 5 μM, prepared in a 1 M KOH solution, or with a 1 M KOH solution to a final concentration of 100 μM as the control. The time course procedure started at time zero with the simultaneous and parallel inoculation of 10 Erlenmeyer flasks containing *Physcomitrella* plant material. Five were treated with the hormone (2iP) and five others treated with the KOH solution as negative controls. A total of 10 inoculations were made within 12 s with a variation of 3 s from one experiment to the next. Two minutes after the beginning of inoculations, two treated Erlenmeyer flasks containing 150 mL of protonema culture were taken simultaneously, and the plant material was harvested through parallel filtration using gauze and suction in a double Büchner funnel (diameter 80 mm) system (self-made) connected to a membrane pump. Afterward, the material was immediately frozen in liquid nitrogen and stored at −80 °C. The total procedure until the sample was frozen in liquid nitrogen took approximately 23 s, with a variation of 5 s from one experiment to the next. The total harvest from each of the Erlenmeyer flasks containing 150 mL of plant material was sufficient for analysis in triplicate. The time course experiment continued at minutes 4, 6, and finally at minute 15. At each of these time points, the previously described procedure was repeated three times.

Extraction of Total Proteins. Total protein extraction was conducted as described earlier.[24] Briefly, 60 mg of ground moss was extracted with 1.9 mL of acetone and 13 mM DTT at room temperature and then stored at −20 °C for 2 h. After centrifugation at 19 000*g* at −10 °C for 15 min, the pellet was washed twice with ice cold acetone and 13 mM DTT and then dried under vacuum for 15 min. Total protein was extracted with 100 μL of 9 M urea, 2% (w/v) CHAPS, and 5 mM TBP with shaking at room temperature for 1 h. Insoluble material was removed by centrifugation at 19 000*g* at room temperature for 15 min. The average protein content was 10 mg/mL determined according to a modified Bradford protocol.[59]

Trypsin Digestion. A total of 1 mg of protein in 100 μL of 9 M urea, 2% CHAPS, and 5 mM TBP was diluted with 1.5 mL of 50 mM NH_4HCO_3 pH 7.8. After the addition of 20 μg of trypsin (≥100U) digestion was performed at 37 °C for 16 h. The reaction was stopped by the addition of formic acid to a final concentration of 5%.

Desalting and Concentration of Total Peptides. Desalting and the concentration of the peptide mixture was accomplished using a combination of two different reverse phase chromatography systems. Self-made chromatography columns were packed with 60 μL of POROS 50 R2 reversed phase packing or 100 μL of oligo R3 reversed phase packing described previously.[24] The peptides were eluted, then dried under vacuum, and finally redissolved in 50 μL of 0.1 M acetic acid before being loaded onto the IMAC column.

Isolation of Phosphopeptides. Phosphopeptides were enriched from the peptide mixture by immobilized metal affinity chromatography (IMAC) using self-made chromatography columns filled with 100 μL of Ni−NTA Superflow (Qiagen) as described earlier.[24] After the peptides were loaded, the column was washed with 600 μL of 100 mM NaCl in 75:25:1 (v:v:v) water/acetonitrile/acetic acid. Following an additional wash step with 200 μL of 0.1 M acetic acid, phosphopeptides were eluted with 500 μL of 50 mM Na_2HPO_4, pH 9.4.

Phosphopeptide Separation. Fractionation of phosphopeptides was performed by reversed phase HPLC. A precolumn (ChromCart, Macherey-Nagel, Düren, Germany Nucleosil, 8/3, 300−5C18) was connected to the analytical HPLC column (Macherey-Nagel, Nucleosil, 300−5 μm, 125 × 2 mm ID) as described previously.[24] A total of 10 fractions was collected every 3 min starting from the wash step to the end of the gradient. The 10 fractions were spiked with 10 fmol of two synthetic phosphorylated peptides PVRRRpSGANYRAY (mass $[M+H]^+$ = 1645.8076) and EAQAApSAAQAK (mass $[M+H]^+$ =1125.4941). The 10 fractions were then dried under vacuum prior to MALDI-TOF-MS phosphopeptides profiling.

Alkaline Phosphatase Treatment. The lyophilised peptides were redissolved in 14 μL of 50 mM NH_4HCO_3, pH 7.8. For MALDI-TOF-MS, alkaline phosphatase treatment was performed as described previously.[24] Briefly, 1.5 μL of the phosphopeptide solution was incubated with 0.05 U/μL alkaline phosphatase at 37 °C for 30 min. For LC-MS/MS, 6.4 μL of the phosphopeptide solution was loaded for analysis. Alkaline phosphatase (0.05 U/μL) was added, and the sample was incubated at 37 °C for 30 min. The sample was then acidified with 0.5 μL of 5% formic acid. The identification of phosphopeptides was achieved in MALDI-TOF-MS by observing the loss of 80Da (due to HPO_3 loss) or multiples of 80Da mass shifts after alkaline phosphatase treatment for multiphosphorylated peptides.

MALDI -TOF-MS, MALDI -TOF-MS/MS, and Phosphopeptide Profiling. MALDI-TOF-MS and MS−MS mass measurements were carried out on an Ultraflex TOF/TOF mass spectrometer (Bruker Daltonik, Bremen, Germany). MS and LIFT spectra were acquired with the Ultraflex TOF/TOF mass spectrometer with gridless ion optics under control of Flexcontrol 2.0. This instrument equipped with the SCOUT High-Resolution Optics with X−Y multisample probe, and a gridless reflector was used at a maximum accelerating potential of 25 kV and was operated in reflector mode. Ionization was accomplished with a 337-nm beam from a nitrogen laser with a repetition rate of 20 Hz. The output signal from the detector was digitized at a sampling rate of 2 GHz.

Both phosphopeptides and dephosphorylated peptide (with alkaline phosphatase) fractions were treated as follows: the samples were prepared by standard dried droplet preparation

on stainless steel MALDI targets and AnchorChip 384-well target plate (Bruker Daltonics) using α-cyano-4-hydroxycinnamic acid (HCCA). The HCCA matrix used was a freshly saturated solution of recrystallized HCCA in acetonitrile and water 50:50 (v:v). Before use, one volume of that HCCA solution was diluted with two volumes of acetonitrile and water 50:50 (v:v). Aliquots (0.5 mL) of sample were spotted onto the target with 0.1 μL of 5% formic acid followed by 0.5 μL of the HCCA matrix solution. External calibration of MALDI mass spectra was carried out using the singly charged monoisotopic peak of four peptides, angiotensin II ($m/z = 1046.542$), substance P ($m/z = 1347.735$), bombesin ($m/z = 1619.822$), and ACTH 18−39 ($m/z = 2465.199$). Monoisotopic peptide masses were automatically annotated using flexAnalysis 2.0 (Bruker Daltonik). The total number of spots analyzed for each round of experiments was 560. Since we had four time points and 10 HPLC fractions for each time point multiplied by two (each time point a cytokinin treatment and a KOH control), we had a total of 80 ($4 \times 10 \times 2 = 80$) phosphopeptide fractions to be analyzed. Additionally, we measured four MALDI preparations (MALDI spots) from each phosphopeptide sample and three MALDI preparations of alkaline phosphatase dephosphorylated peptide samples, making a total of 560 ($80 \times (4 + 3) = 560$). The overall procedure was repeated in triplicate consecutive analysis (3 days). For each MALDI spot, 1000 spectra were acquired (50 laser shots at 20 different spot positions). All signals with a signal-to-noise (S/N) ratio >3 in the mass range of 450−4000 Da were recorded using the AutoXecute tool of the flexControl 2.0 (Bruker Daltonik) acquisition software for peptide pattern recognition. All peptide patterns were checked manually. To that purpose, we determined the variation in the m/z ratios, and we compared relative and absolute peak intensities of at least 10 selected signals within a same fraction including the two internal standard synthetic peptides. The mass spectra from the repeat experiments were compared and we accepted a S/N ratio >3 in mass range and a mass error no more than 20 ppm. We accepted a variation coefficient (CV) of 24%. All of the mass spectra that did not meet these criteria were rejected (5.3%). This value indicates that typical quantification errors from mass spectrometry were smaller than our selected conservative threshold chosen for biological significance. We counted peaks in the mass spectra from controls and cytokinin-treated fractions which showed reproducible increases/decreases. From this, we chose three as a conservative threshold for biological significance. This threshold represents a phosphopeptide that is quantitatively affected by cytokinin stimulation. This threshold prevented us from false data interpretation. We also counted peaks that newly appeared and also disappeared in the mass spectra of cytokinin treated fractions versus control. A new peak either corresponds to a new phosphopeptide which before cytokinin stimulation was not phosphorylated and therefore not purified by IMAC, or a new peak may also represent a change in the phosphorylation state of a previously phosphorylated peptide characterized by a different m/z before cytokinin stimulation. The phosphopeptides and the dephosphorylated peptides were then sequenced by MALDI-TOF-MS/MS.(Ultraflex TOF-TOF mass spectrometer Bruker Daltonik, Bremen, Germany).The LIFT-MS/MS spectra were obtained by the analysis of the metastable ions, generated by laser-induced decomposition (LID) of the selected precusor ions. No additional collision gas was applied. Precursor ions were accelerated to 8 kV and selected in a timed ion gate. The fragments were further accelerated by 19 kV in the LIFT cell and their masses were analyzed after the ion reflector passage. LIFT-MS/MS spectra were annotated with the Biotools 2.2 (Bruker Daltonik) software package. A high-energy CID mode was used to enhance intensities of fragments in the low fragment mass range; a collision gas, argon, was introduced to increase the source pressure to 6×10^{-6} mbar. All of the MS/MS spectra were interpreted manually. The resulting amino acid sequences obtained are represented in bold (Table 1 and Table 1 in the Supporting Information).

NanoLC-MS/MS and Data Interpretation. NanoLC-MS/MS analysis of the tryptic phosphopeptides was performed using a CapLC capillary LC system (Micromass) coupled to a hybrid quadrupole orthogonal acceleration time-of-flight tandem mass spectrometer (Q-TOF II, Micromass, Manchester, U.K.) fitted with a Z-spray nanoflow electrospray ion source. Chromatographic separations were conducted on a Pepmap C18 75 μm i.d. × 15 cm length, reverse phase (RP) capillary column (LC Packings, Sunnyvale, CA) with a flow rate of 200 nL min^{-1} accomplished by a precolumn split. An external calibration was performed using a 2 pmol μL^{-1} GFP ((Glu^1)-Fibrinopeptide B) solution. The mass spectrometer was operated in positive ion mode with a potential of 3500 V applied to the nanoflow probe body. The collision energy was determined on the fly based on the mass and charge state of the peptide. Charge state recognition was used to switch only mono, doubly, and triply charged ions into MS/MS mode. Mass data acquisition was piloted by MassLynx 4 software (Micromass) using automatic switching between MS and MS/MS modes. Phosphopeptide samples (6.4 μL; dephosphorylated or not by alkaline phosphatase treatment) were injected. For the phosphopeptides responsive to cytokinin determined by MALDI-TOF-MS phosphopeptide profiling, the corresponding monoisotopic peptide masses were used to calculate doubly and triply charged ions of the corresponding phosphorylated and dephosphorylated candidate peptides. The ions were used to create a MS and MS/MS priority sequencing list.

Mass spectra data collected during LC-MS/MS analysis was processed and converted into PKL files to be submitted to the local search software MASCOT 2.0 (Matrix Science, London, U.K.) for *P. patens* EST/contig/ raw genomic database searches. The peak list was created using the ProteinLynx 4.0 software (Micromass). The searches were done with a tolerance on mass measurement of 0.25 Da in MS mode and 0.3 Da in MS/MS mode. These searches did not always lead to positive identification since the *P. patens* genome has not yet been fully sequenced. Therefore, peptide de novo sequencing was necessary for successful identification. The de novo interpretation of the MS/MS spectra was performed with the PEAKS 2_3 Studio software (Bioinformatics Solutions, Waterloo, Canada). The sequencing mass tolerance was of 0.25 Da. Confidence of the amino acid tag was set to 90% and verified manually

The MS/MS spectra of the phosphorylated peptides were mostly poorly informative. Manual sequencing was also made (on dephosphorylated peptides) using PepSeq 4.0 software (Micromass). The intensity threshold was set to 1%, and the fragmentation tolerance was 0.25 Da for monoisotopic ions. Molecular weight tolerance was 0.25 Da. The amino acid tags obtained were subsequently used to interrogate the different *P. patens* EST/contig databases (http://www.cosmoss.org/) and available raw genomic data present in NCBI (National Center for Biotechnology) using tblastn. The tblastn program has been used to compare the single peptide tag query sequence against the *P. patens* nucleotide sequence database dynamically trans-

lated in all reading frames. The different I/L K/Q possibilities have been tried. The "expected" value represents the statistical significance threshold for reporting matches against database sequences; the default value was $1e^{+4}$ for our single peptide FASTA searches. No filter was set, the substitution matrix used was BLOSUM 62, and the un-gapped alignment mode has been performed. The *P. patens* EST/contig sequences that matched perfectly with the *P. patens* phosphopeptide sequences were retained. If full match was not guarantied, the ESTs/contigs with the highest sequence coverage with the phosphopeptide tag were retained. Thus, the hits with a minimum of 70% of the peptide sequence coverage were also retained.

The *P. patens* EST/contig or genomic information matching with the single peptide tag were then used as query for protein identification accomplished by homology searches with proteins present in the NCBI (National Center for Biotechnology) nonredundant protein databases (http://www.ncbi.nlm.nih.gov/blast/). The overall procedure of EST/contig identification and protein annotation was run on Cosmoss (http://www.cosmoss.org/). The statistical evaluation of the results and the validation of the matches was performed manually as described earlier.[60−62] Several different predictive bioinformatic tools have been tested on the EST/contigs coding for proteins with unknown function and MOPPs. InterPro (http://www.ebi.ac.uk/interpro/) and Pfam (http://www.sanger.ac.uk/Software/Pfam/ind ex.shtml). ChloroP 1.1 Prediction server (http://www.cbs-.dtu.dk/services/ChloroP/). TargetP 1.1 server (http://www.cbs.dtu.dk/services/TargetP/). TMHMM 2.0 server (http://www.cbs.dtu.dk/services/TMHMM/). The obtained peptides were also run against the phospho-predictor site NetPhos (www.cbs.dtu.dk/services/Net-Phos, Table 3, in the Supporting Information)

Abbreviations

P. patens, Physcomitrella patens; EST, expressed sequence tags; GPDH, glyceraldehyde−3-phosphate dehydrogenase; BLAST, basic local alignment search tool; Rubisco, lsu, ribulose bisphosphate carboxylase large subunit; CHAPS, 3-[(3-cholamidopropyl)-dimethylammonio]-1-propane sulfonate; TBP, tributyl phosphine; MOPP, moss phosphorylated protein; 2iP, 6-(γ-γ)-dimethylallylaminopurine; PTM, posttranslational modification; CV, variation coeficient; CID, collision induced dissociation; NO, nitric oxide.

Acknowledgment. The authors thank Sandra Richardt (Freiburg University) for helping with plant cell culture, Pr. Dr. Thomas J. Bach (IBMP, Strasbourg University) and Dr. Fabrice Bertile (LSMBO, Strasbourg University) for suggestions, discussions, and helpful comments, and Dr. Andreas Tholey (Saarland University) for the gift of the phosphorylated synthetic standard peptides. Financial support by DFG to R.R. (Re 837) and to E.S. (Sa 1014) is gratefully acknowledged

Supporting Information Available: Supplimentary tables and figures. This material is available free at http:/pubs.acs.org.

References

(1) Inoue, T.; Higuchi, M.; Hashimoto, Y.; Seki, M.; Kobayashi, M., Kato, T.; Tabata, S.; Shinozaki, K.; Kakimoto, T. *Nature* **2001**, *409*, 1060−1063.
(2) Ueguchi, C.; Koizumi, H.; Suzuki, T.; Mizumo, T. *Plant Cell Physiol.* **2001**, *42*, 231−235.
(3) Kakimoto, T. *Plant Cell Physiol.* **2001**, *42*, 677−685.
(4) Reski, R.; Reynolds, S.; Wehe, M.; Kleber-Janke, T.; Kruse S. *Bot. Acta* **1998**, *111*, 1−15.
(5) Kasten, B.; Buck, F.; Nuske, J.; Reski, R. *Planta* **1997**, *201* (3), 261−72.
(6) Schumaker, K. S.; Dietriech, M. A. Rev. *Plant Physiol. Plant Mol. Biol.* **1998**, *49*, 501−23.
(7) Reski, R. *Trends Plant Sci.* **1998**, *6*, 209−210.
(8) Schaefer, D. G. *Curr. Opin. Plant Biol.* **2001**, *4*, 143−150.
(9) Strepp, R.; Scholz, S.; Kruse, S.; Speth, V.; Reski, R. *Proc. Natl. Acad. Sci. U.S.A.* **1998**, *95*, 4368−4373.
(10) Imaizumi, T.; Kadota, A.; Hasebe, M.; Wada, M. *Plant Cell* **2002**, *14*, 373−388.
(11) Hohe, A.; Reski, R. *Plant Sci.* **2002**, *163*, 69−74.
(12) Hohe, A.; Decker, E. L.; Gorr, G.; Schween, G.; Reski, R. *Plant Cell Rep.* **2002**, *20*, 1135−1140.
(13) Mann, M.; Jensen, O. N. *Nat. Biotechnol.* **2003**, *21*, 255−261.
(14) Hunter, T. *Cell* **2000**, *100*, 113−127.
(15) Jensen, O. N. *Curr. Opin. Chem. Biol.* **2004**, *8*, 33−41.
(16) Blagoev, B.; Ong, S. E.; Kratchmarova, I.; Mann, M. *Nat. Biotechnol.* **2004**, *22* (9), 1139−1145.
(17) Rush, J.; Moritz, A.; Lee, K. A,; Guo, A.; Goss, V. L.; Spek, E. J.; Zhang, H.; Zha., X. M.; Polakiewicz, R. D.; Comb, M. J. *Nat. Biotechnol.* **2005**, *23* (1), 94−101.
(18) Ficarro, S. B.; McCleland, M. L.; Stukenberg, P. T.; Burke, D. J.; Ross, M. M.; Shabanowitz, J.; Hunt, D. F.; White, F. M. *Nat. Biotechnol.* **2002**, *19*, 301−305.
(19) Ficarro, S. B.; Chertinihin, O.; Westbrook, A.; White, F.; Jayes, F.; Kalab, P.; Marto, J. A.; Shabanowitz, J.; Herr, J. C.; Hunt, D. F.; Visconti, P. E. *J. Biol. Chem.* **2003**, *278*, 11579−11589.
(20) Brill, L. M.; Salomon, A. R.; Ficarro, S. B.; Mukherji, M.; Stetter-Gill, M.; Peters, E. C. *Anal. Chem.* **2004**, *76*, 2763−2772.
(21) Collins, M. O.; Yu, L.; Coba, M. P.; Husi, H.; Campuzano, I.; Blackstock, W. P.; Choudhary, J. S.; Grant, S. G. *J. Biol. Chem.* **2005**, *280*, 5972−5982.
(22) Nühse, T. O.; Stensballe, A.; Jensen, O. N.; Peck, S. C. *Mol. Cell. Proteomics* **2003**, *2*, 1234−1243.
(23) Gruhler, A.; Olsen, J. V.; Mohammed, S.; Mortensen, P.; Faergeman, N. J.; Mann, M.; Jensen, O. N. *Mol. Cell. Proteomics* **2005**, *4*, 310−327.
(24) Heintz, D.; Wurtz, V.; High, A. A.; Van Dorsselaer, A.; Reski, R.; Sarnighausen, E. *Electrophoresis* **2004**, *25*, 1149−1159.
(25) Leipzig, J.; Pevzner, P.; Heber, S. *Nucleic Acid Res.* **2004**, *32*, 3977−83.
(26) Ma, B.; Zhang, K.; Hendrie, C.; Liang, C.; Li, M.; Doherty-Kirby, A.; Lajoie, G. *Rapid Commun. Mass Spectrom.* **2003**,*17*, 2337−42.
(27) Loughrey Chen, S.; Huddleston, M. J.; Shou, W.; Deshaies, R. J.; Annan, R. S.; Carr, S. A. *Mol. Cell. Proteomics* **2002**, *1*, 186−196.
(28) Mann, M.; Wilm, M. *Anal. Chem.* **1994**, *66*, 4390−4399.
(29) Carr, S. A.; Huddleston, M. J.; Annan, R. S. *Anal. Biochem.* **1996**, *229*, 180−192.
(30) Janek, K.; Wenschuh, H.; Bienert, M.; Krause, E. *Rapid Comm. Mass Spectrom.* **2001**, *15*, 1593−1599.
(31) Klem, C.; Schroeder, S.; Gluckmann, M.; Beyermann, M.; Krause, E. *Rapid Comm. Mass Spectrom.* **2004**, *18*, 2697−2705.
(32) Rensing, S. A.; Rombauts, S.; Hohe, A.; Lang, D.; Duwenig, E.; Rouzé, P.; Van de Peer, Y.; Reski, R. http://www.plant-biotech-.net/Rensing_et_al_transcriptome2002.pdf, 2002.
(33) Rensing, S. A.; Rombauts, S.; Van de Peer, Y.; Reski, R. *Trends Plant Sci.* **2002**, *7*, 535−538.
(34) Rensing, S. A.; Fritzowsky, D.; Lang, D.; Reski, R. *BMC Genomics* **2004**, *6*, 43.
(35) Nishiyama, T.; Fujita, T.; Shin-I, T.; Seki, M.; Nishide, H.; Uchiyama, I.; Kamiya, A.; Carninci, P.; Hayashizaki, Y.; Shinozaki, K.; Kohara, Y.; Hasebe, M. *Proc. Natl. Acad. Sci. U.S.A.* **2003**, *100*, 8007−8012.
(36) Lang, D.; Eisinger, J., Reski, R., Rensing, R. *Plant Biol.* **2005**, *7*, 238−250.
(37) Duncan, M. W.; Matanovic, G.; Cerpa-Poljak, A. *Rapid Commun. Mass Spectrom.* **1993**, *7*, 1090−1094.
(38) Tun, N. N.; Holk, A.; Scherer, G. F. E. *FEBS Lett.* **2001**, *509*, 174−176.
(39) D'Agostino, B.; Deruère, Y.; Kieber, J. *J. Plant Physiol.* **2000**, *124*, 1706−1717.
(40) Brenner, W. G.; Romanov, G. A.; Köllmer, I.; Bürkle, L.; Schmülling, T. *Plant J.* **2005**, *44*, 314−33.
(41) Romanov, G. A.; Kieber, J. J.; Schmülling, T. *FEBS Lett.* **2002**, *515*, 39−43.

(42) Kulaeva, O. N.; Karavaito, N. N.; Selivankina, S. Yu.; Kusnetsov, V. V.; Zemlyachenko., Ya. V,; Cherepneva, G. N.; Maslova, G. G.; Lukevich, T. V.; Smith, A. R.; Hall, M. A. *Plant Growth Regul.* **2000**, *32*, 329−335.
(43) Klumpp, S.; Krieglstein, J. *Eur. J. Biochem.* **2002**, *269*, 4, 1067−71.
(44) Benkova, E.; Witters, E.; van Dongen, W.; Kolar, J.; Motyka V.; Brzobohaty, B.; Van Onckelen, H. A.; Machackova, I. *Plant Physiol.* **1999**, *121*, 245−251.
(45) Lyukevich, T. V.; Kustenov, V. V.; Karavaiko, N. N.; Selivankina, S. Yu.; Kulaeva, O. N. *Fiziol. Rast.* **2002**, *49*, 105−112.
(46) Spiro, M. D.; Torabi, B.; Cornell, C. N. *Plant Cell Physiol.* **2004**, *45*, 1252−60.
(47) Smets, R.; Le, J., Prinsen, E.; Verbelen, J. P.; Van Onckelen, H. A. *Planta* **2005**, *221*, 39−47.
(48) Sweere, U.; Eichenberg, K.; Lohrmann, J.; Mira-Ronaldo, V.; Baurle, I.; Kudla, J., Nagy, F.; Schafer, E.; Harter, K. *Science* **2001**, *294*, 1108−1111.
(49) Chory, J.; Reinecke, D.; Sim, S.; Wasburn, T.; Brenner, M. *Plant Physiol.* **1994**, *104*, 339−347.
(50) Yong, J. W.; Wong, S. C.; Letham, D. S.; Hocart, C. H.; Farquhar, G. D. *Plant Physiol.* **2000**, *124*, 767−779.
(51) Snell, K.; Baumann U.; Byrne P. C.; Chave K. J. *Adv. Enzyme Regul.* **2000**, *40*, 353−403.
(52) Trivedi, V.; Gupta, A.; Jala, V. R.; Saravanan, P., Rao, G. S.; Rao, N. A.; Savithri, H. S.; Subramanya, H. S. *J. Biol. Chem.* **2002**, *277*, 17161−17169.
(53) Kenyon, S. H.; Ast, T.; Gibbons, W. A. *Biochem. Soc. Trans.* **1995**, *2*, 335−39.
(54) Smalle, J.; Kurepa, J.; Yang, P.; Babiychuk, E.; Kushnir, S.; Durski, A.; Viestra, R. D. *Plant Cell* **2002**, *14*, 17−32.
(55) Huang, X. Y.; Barrios, L. A. M.; von Khorporn, P.; Honda, S.; Albertson, D. G.; Hecht, R. M. *J. Mol. Biol.* **1989**, *206*, 411−424.
(56) Dugaiczyk, A.; Haron, J. A.; Stone, E. M.; Dennison, O. E.; Rothblum K. N.; Schwartz R. J. *Biochemistry* **1983**, *22*, 1605−1613.
(57) Berry, M. D.; Boulton, A. A. *J. Neurosci. Res.* **2000,** *60*, 150−154.
(58) Franco-Zorrilla, J. M.; Martin, A. C.; Leyva, A.; Paz-Ares, J. *Plant Physiol.* **2005**, *138*, 847−857.
(59) Ramagli, L. S.; Rodriguez, L. V. *Electrophoresis* **1985**, *6*, 559−563.
(60) Karlin, S.; Altschul, S. F. *Proc. Natl. Acad. Sci. U. S. A.* **1990**, *6*, 2264−8.
(61) Rensing, S. A.; Fritzowsky, D.; Lang, D.; Reski, R. *BMC Genomics* **2005**, *1*, 43.
(62) Lang, D.; Eisinger, J.; Reski, R.; Rensing, S. A. *Plant Biol.* **2005**, *7*, 238−50.
(63) Zapponi, M. C.; Iadarola, P.; Stoppini, M.; Ferri, G. *Biol. Chem. Hoppe Seyler* **1993**, *6*, 395−402.
(64) Yang, E. J.; Oh, Y. A.; Lee, E. S.; Park, A. R.; Cho, S. K.; Yoo, Y. J, Park, O. K. *Biochem. Biophys. Res. Commun.* **2003**, *4*, 862−8.

PR060152E